PHYSICAL REVIEW D **96,** 094030 (2017)

Hidden bottom pentaquark states with spin 3/2 and 5/2

K. Azizi,[1,2] Y. Sarac,[3] and H. Sundu[4]

[1]*Physics Department, Doğuş University, Acıbadem-Kadıköy, 34722 Istanbul, Turkey*
[2]*School of Physics, Institute for Research in Fundamental Sciences (IPM), P.O. Box 19395-5531 Tehran, Iran*
[3]*Electrical and Electronics Engineering Department, Atilim University, 06836 Ankara, Turkey*
[4]*Department of Physics, Kocaeli University, 41380 Izmit, Turkey*

(Received 5 July 2017; published 29 November 2017)

Theoretical investigations of the pentaquark states that were recently discovered provide important information on their nature and structure. It is necessary to study the spectroscopic parameters, like masses and residues of particles belong to the class of pentaquarks, and ones having similar structures. The mass and pole residue are quantities that emerge as the main input parameters in exploration of the electromagnetic strong and weak interactions of the pentaquarks with other hadrons in many frameworks. This work deals with a QCD sum rule analysis of the spin-3/2 and spin-5/2 bottom pentaquarks with both positive and negative parities aiming to evaluate their masses and residues. In calculations, the pentaquark states are modeled by molecular-type interpolating currents: for particles with $J = 5/2$, a mixing current is used. We compare the results obtained in this work with the existing predictions of other theoretical studies. The predictions on the masses may shed light on experimental searches of the bottom pentaquarks.

DOI: 10.1103/PhysRevD.96.094030

I. INTRODUCTION

The announcement by the LHCb Collaboration [1] on the observation of the two charmed pentaquark states placed the subject under the spotlight in both theoretical and experimental sides. The nonconventional internal quark structure of these states, which are excluded neither by the naive quark model nor by QCD, puts them at the focus of increasing interest. Many experimental studies have been conducted to prove the existence of these particles, as well as to explore their internal structures. Parallel theoretical studies on the nature of these exotic baryons are in progress.

The experimental searches for the pentaquark states have a long and controversial story. We refrain from listing all those searches and refer the reader to Ref. [2] and references therein for a full history. Although their existence was predicted many decades ago by Jaffe [3] and their properties were worked out in many theoretical studies (see, for instance, Refs. [4–14]), the searches on the pentaquarks ended up in positive results recently and the two pentaquark states $P_c^+(4380)$ and $P_c^+(4450)$ were reported by the LHCb Collaboration in 2015 in the $\Lambda_b^0 \to J/\psi K^- p$ decays with masses $4380 \pm 8 \pm 29$ and $4449.8 \pm 1.7 \pm 2.5$ MeV, spins $3/2$ and $5/2$, and decay widths $205 \pm 18 \pm 86$ and $39 \pm 5 \pm 19$ MeV, respectively [1]. There are other states which are interpreted as other possible pentaquark states. In Refs. [15] some of the newly observed Ω_c states by LHCb [16] were considered among possible pentaquark states. Also, in Ref. [17] the states $N(1875)$ and $N(2100)$ were stated to be possible strange partners of $P_c^+(4380)$ and $P_c^+(4450)$, respectively.

The observation of LHCb boosted intense theoretical works to provide an explanation of the properties of these states. Via different models, such as the diquark-triquark model [18–20], diquark-diquark-antiquark model [18,21–26], meson baryon molecular model [18,27–36], and topological soliton model [37], their properties and substructures were investigated. A review on the multiquark states including pentaquarks and their possible experimental measurements can be found in Ref. [38]. Some of the recent investigations have considered other possible substructures for the pentaquark states. Besides the mass of the hidden-charmed molecular pentaquark states, the mass of charmed-strange molecular pentaquark states, and other hidden-charmed molecular pentaquark states, which are named $P_c'(4520)$, $P_c'(4460)$, $P_{cs}(3340)$, and $P_{cs}(3400)$, were predicted in Ref. [34]. The same work also contains the predictions on the masses of hidden bottom pentaquark states with molecular structure. In Ref. [39], besides the $P_c^+(4380)$ state, the possible existence of hidden bottom pentaquarks with a mass around 11080–11110 MeV and quantum numbers $J^P = 3/2^-$ was emphasized, and it was indicated that there may exist some loosely bound molecular-type pentaquarks with heavy quark contents $c\bar{b}$, $b\bar{c}$, or $b\bar{b}$. For such type of pentaquark states, the mass predictions were presented in Ref. [40]. In this work, using a variant of D4–D8 brane model [41], the mass of charmed and bottom pentaquarks were predicted as $M_{\bar{c}c} = 4678$, $M_{\bar{c}b} = M_{\bar{b}c} = 8087$, and $M_{\bar{b}b} = 11496$ MeV. See also Refs. [42,43] for more information on the properties of the charmed and bottom pentaquark states using the coupled-channel unitary approach as well as [44–47] on the structure of the pentaquarks and triangle singularities.

In light of all these developments, it is necessary to explore the pentaquarks to gain constructive information on their nature and substructures. If one considers the historical development of the particle physics, the observations of the particles are sequential. The observation of baryons containing a c quark was followed by the observation of similar baryons containing a b quark. Therefore, it is natural to expect a possible subsequent observation of the bottom analogues of the observed pentaquark states. Investigations of their spectroscopic and electromagnetic properties, as well as their strong and weak decays supply beneficial information for the future experimental searches. In addition to this, further theoretical studies are helpful to get insights into the nature of these particles, as well as into the dynamics of their strong interactions by comparing the results with the existing theoretical predictions and experimental data. Starting from this motivation, in this work, we extend our previous study on the properties of charmed pentaquarks [2] and calculate the masses and residues of the pentaquark states P_b with $J = 3/2$ and $J = 5/2$ by considering both the positive and negative parity states. For this purpose, we use the QCD sum rule method [48,49], interpolating currents of the molecular form for the states with $J = 3/2$ and a mixed molecular current for those states having $J = 5/2$. For the latter, we optimize the mixing angle according to the standard prescriptions.

The present work is organized in the following way. In Sec. II, calculations of the mass and residue of hidden bottom pentaquark states are presented. Section III, is devoted to the numerical analysis and discussion on the obtained results. In Sec. IV, we summarize our results and briefly discuss prospects to study decays of the pentaquark states. Some spectral densities used in calculations are moved to the Appendix.

II. HIDDEN BOTTOM PENTAQUARK STATES WITH $J = 3/2$ AND $J = 5/2$

This section presents the calculations of the masses and residues of the hidden bottom pentaquark states with $J = 3/2$ and $J = 5/2$. In both cases, we consider the positive and negative parity states. To begin the calculations, for the state with $J = 3/2$ we use the following two-point correlation function:

$$\Pi_{\mu\nu}(p) = i \int d^4x e^{ip\cdot x} \langle 0|\mathcal{T}\{J_\mu^{\bar{B}^*\Sigma_b}(x)\bar{J}_\nu^{\bar{B}^*\Sigma_b}(0)\}|0\rangle, \quad (1)$$

where $J_\mu^{\bar{B}^*\Sigma_b}(x)$ is the interpolating current having the quantum numbers $J = \frac{3}{2}^-$ [33]. This current couples to both the negative and positive parity particles, and its explicit expression is given as

$$J_\mu^{\bar{B}^*\Sigma_b} = [\bar{b}_d\gamma_\mu d_d][\epsilon_{abc}(u_a^T C\gamma_\theta u_b)\gamma^\theta\gamma_5 b_c]. \quad (2)$$

For the states with $J = 5/2$, the correlation function has the following form:

$$\Pi_{\mu\nu\rho\sigma}(p) = i \int d^4x e^{ip\cdot x} \langle 0|\mathcal{T}\{J_{\mu\nu}(x)\bar{J}_{\rho\sigma}(0)\}|0\rangle, \quad (3)$$

where $J_{\mu\nu}(x)$ is the interpolating current, which also couples to both the positive and negative parity states. This current is chosen as a mixed current composed of $J_{\mu\nu}^{\bar{B}\Sigma_b^*}$ and $J_{\mu\nu}^{\bar{B}^*\Lambda_b}$ [33],

$$J_{\mu\nu}(x) = \sin\theta \times J_{\mu\nu}^{\bar{B}\Sigma_b^*} + \cos\theta \times J_{\mu\nu}^{\bar{B}^*\Lambda_b}, \quad (4)$$

where θ is a mixing angle that should be fixed, and

$$\begin{aligned} J_{\mu\nu}^{\bar{B}\Sigma_b^*} &= [\bar{b}_d\gamma_\mu\gamma_5 d_d][\epsilon_{abc}(u_a^T C\gamma_\nu u_b)b_c] + \{\mu \leftrightarrow \nu\}, \\ J_{\mu\nu}^{\bar{B}^*\Lambda_b} &= [\bar{b}_d\gamma_\mu u_d][\epsilon_{abc}(u_a^T C\gamma_\nu\gamma_5 d_b)b_c] + \{\mu \leftrightarrow \nu\}. \end{aligned} \quad (5)$$

The above correlation functions are calculated in two different ways. On the side of phenomenology, one inserts a complete set of hadronic states with the same quantum numbers as the interpolating currents into the correlation functions. This calculation comes up with results containing hadronic degrees of freedom such as masses and residues. On the QCD side, the same correlation functions are calculated in terms of QCD degrees of freedom. Finally, the coefficients of the same Lorentz structures obtained in both sides are matched and QCD sum rules for the desired physical parameters are obtained.

In the case of states with $J = 3/2$, the procedure summarized above for the physical side leads to the result

$$\begin{aligned} \Pi_{\mu\nu}^{\text{Phys}}(p) &= \frac{\langle 0|J_\mu|\frac{3}{2}^+(p)\rangle\langle\frac{3}{2}^+(p)|\bar{J}_\nu|0\rangle}{m_{\frac{3}{2}^+}^2 - p^2} \\ &+ \frac{\langle 0|J_\mu|\frac{3}{2}^-(p)\rangle\langle\frac{3}{2}^-(p)|\bar{J}_\nu|0\rangle}{m_{\frac{3}{2}^-}^2 - p^2} + \cdots, \end{aligned} \quad (6)$$

where $m_{\frac{3}{2}^+}$ and $m_{\frac{3}{2}^-}$ are the masses of the positive and negative parity particles, respectively. The contributions of the higher states and continuum are represented by the ellipsis in the last equation. The matrix elements in Eq. (6) are given in terms of the residues $\lambda_{\frac{3}{2}^+}$ and $\lambda_{\frac{3}{2}^-}$, and corresponding spinors as

$$\begin{aligned} \langle 0|J_\mu|\frac{3}{2}^+(p)\rangle &= \lambda_{\frac{3}{2}^+}\gamma_5 u_\mu(p), \\ \langle 0|J_\mu|\frac{3}{2}^-(p)\rangle &= \lambda_{\frac{3}{2}^-} u_\mu(p). \end{aligned} \quad (7)$$

A similar result for the correlation function corresponding to $J = 5/2$ states is obtained

$$\Pi^{\rm Phys}_{\mu\nu\rho\sigma}(p) = \frac{\langle 0|J_{\mu\nu}|\frac{5}{2}^+(p)\rangle\langle\frac{5}{2}^+(p)|\bar{J}_{\rho\sigma}|0\rangle}{m^2_{\frac{5}{2}^+}-p^2} + \frac{\langle 0|J_{\mu\nu}|\frac{5}{2}^-(p)\rangle\langle\frac{5}{2}^-(p)|\bar{J}_{\rho\sigma}|0\rangle}{m^2_{\frac{5}{2}^-}-p^2} + \cdots, \quad (8)$$

with the matrix elements defined as

$$\langle 0|J_{\mu\nu}|\frac{5}{2}^+(p)\rangle = \lambda_{\frac{5}{2}^+}u_{\mu\nu}(p),$$
$$\langle 0|J_{\mu\nu}|\frac{5}{2}^-(p)\rangle = \lambda_{\frac{5}{2}^-}\gamma_5 u_{\mu\nu}(p). \quad (9)$$

In these equations $m_{\frac{5}{2}^+}$ and $m_{\frac{5}{2}^-}$ are the masses of the spin-$\frac{5}{2}$ states having positive and negative parities, respectively. Using the matrix elements parameterized in terms of the masses and residues and performing the Borel transformation, the physical side is found as

$$\mathcal{B}_{p^2}\Pi^{\rm Phys}_{\mu\nu}(p) = -\lambda^2_{\frac{3}{2}^+}e^{-\frac{m^2_{\frac{3}{2}^+}}{M^2}}(-\gamma_5)(\not{p}+m_{\frac{3}{2}^+})g_{\mu\nu}\gamma_5 - \lambda^2_{\frac{3}{2}^-}e^{-\frac{m^2_{\frac{3}{2}^-}}{M^2}}(\not{p}+m_{\frac{3}{2}^-})g_{\mu\nu}+\cdots, \quad (10)$$

for pentaquark states with spin-3/2, with M^2 being the Borel parameter. Here, $g_{\mu\nu}$ and $\not{p}g_{\mu\nu}$ are structures that give contributions to only the spin-3/2 particles. By choosing these structures, we eliminate the unwanted spin-1/2 pollution. In the case of hidden bottom pentaquarks with spin-5/2, we find

$$\mathcal{B}_{p^2}\Pi^{\rm Phys}_{\mu\nu\rho\sigma}(p) = \lambda^2_{\frac{5}{2}^+}e^{-\frac{m^2_{\frac{5}{2}^+}}{M^2}}(\not{p}+m_{\frac{5}{2}^+})\left(\frac{g_{\mu\rho}g_{\nu\sigma}+g_{\mu\sigma}g_{\nu\rho}}{2}\right) + \lambda^2_{\frac{5}{2}^-}e^{-\frac{m^2_{\frac{5}{2}^-}}{M^2}}(\not{p}-m_{\frac{5}{2}^-})\left(\frac{g_{\mu\rho}g_{\nu\sigma}+g_{\mu\sigma}g_{\nu\rho}}{2}\right) + \cdots, \quad (11)$$

where we kept again only the structures that give contributions to the spin-5/2 particles and ignored other structures giving contributions to the spin-3/2 and spin-1/2 particles.

The calculation of the correlation function in terms of QCD degrees of freedom is the next stage of the calculations. In this part, the interpolating currents of the interested states are substituted into the correlation functions and the quark fields are contracted through Wick's theorem. This procedure ends up finding the correlation functions in terms of the light and heavy quark propagators. Using the quark propagators in coordinate space as presented in [2], we apply the Fourier transformation to transfer the calculations to the momentum space. To suppress the contributions of the higher states and continuum we apply the Borel transformation as well as continuum subtraction and use the dispersion integral representation. At the end of this procedure, we obtain the spectral densities as the imaginary parts of the functions corresponding to all selected structures.

The calculations of physical and theoretical sides are followed by the selection of the coefficients of the same structures from both sides and their matching to obtain the relevant QCD sum rules that will give us the physical quantities of interest. The final forms of the sum rules are obtained as

$$m_{J^+}\lambda^2_{J^+}e^{-m^2_{J^+}/M^2} - m_{J^-}\lambda^2_{J^-}e^{-m^2_{J^-}/M^2} = \Pi^m_J,$$
$$\lambda^2_{J^+}e^{-m^2_{J^+}/M^2} + \lambda^2_{J^-}e^{-m^2_{J^-}/M^2} = s_J\Pi^p_J, \quad (12)$$

where $J = 3/2$ or $5/2$. In the last equation, s_J equals -1 for $3/2$ and 1 for $5/2$ states. The functions $\Pi^m_{3/2}$, $\Pi^p_{3/2}$, $\Pi^m_{5/2}$, and $\Pi^p_{5/2}$ are coefficients of the structures $g_{\mu\nu}$, $\not{p}g_{\mu\nu}$, $(g_{\mu\rho}g_{\nu\sigma}+g_{\mu\sigma}g_{\nu\rho})/2$, and $\not{p}(g_{\mu\rho}g_{\nu\sigma}+g_{\mu\sigma}g_{\nu\rho})/2$, respectively, on the side of QCD. These functions are written in terms of the spectral densities as

$$\Pi^j_J = \int_{4m_b^2}^{s_0} ds\rho^j_J(s)e^{-s/M2}, \quad (13)$$

where $j = m$ or p. The spectral densities can also be written in terms of the perturbative and nonperturbative parts as

$$\rho^j_J(s) = \rho^{\rm j,pert}_J(s) + \sum_{k=3}^{6}\rho^j_{J,k}(s), \quad (14)$$

where $\rho^j_{J,k}(s)$ represents the nonperturbative contributions to the spectral densities. As examples, we present the perturbative and nonperturbative parts of the spectral densities corresponding to the structures $g_{\mu\nu}$ and $(g_{\mu\rho}g_{\nu\sigma}+g_{\mu\sigma}g_{\nu\rho})/2$ in terms of the integrals over the Feynman parameters x and y in the Appendix.

As is seen, the sum rules contain four unknowns in each case which include the masses and residues of considered states. We need two extra equations in each case that are obtained by applying a derivative with respect to $\frac{1}{M^2}$ to both sides of the above equations. By simultaneous solving of the obtained equations' sets, one can obtain the masses and residues of the particles with both parities in terms of the QCD degrees of freedom as well the Borel parameter, continuum threshold, and mixing angle in the case of spin-5/2 particles.

III. NUMERICAL RESULTS

The input parameters that are needed in the numerical analyses of the obtained sum rules in the previous section are collected in Table I. Note that, in the numerical

TABLE I. Some input parameters used in the calculations.

Parameters	Values
m_b	(4.78 ± 0.06) GeV
$\langle \bar{q}q \rangle$	$(-0.24 \pm 0.01)^3$ GeV^3
m_0^2	(0.8 ± 0.1) GeV^2
$\langle \bar{q}g_s\sigma Gq \rangle$	$m_0^2\langle \bar{q}q \rangle$
$\langle \frac{\alpha_s G^2}{\pi} \rangle$	(0.012 ± 0.004) GeV^4

calculations, we use the b quark pole mass and the masses of light u and d quarks are taken as zero. It is well known that the parameters of the bottom systems depend on the b quark mass, considerably. However, our numerical analyses show that the results of physical quantities under consideration show more stability with respect to the changes of the auxiliary parameters when the b quark pole mass is used compared to the one when the b quark running mass in the $\overline{\text{MS}}$ scheme is taken into account. Our analyses also show that when we use the b quark pole mass we achieve higher pole contributions in all channels compared to the case of b quark running mass. Therefore, we choose the b quark pole mass to numerically analyze the obtained sum rules.

The next step is to determine the working intervals for two auxiliary parameters, namely, the continuum threshold s_0 and the Borel parameter M^2. For the determination of the Borel window, the convergence of the series of operator product expansion (OPE) and the adequate suppression of the contributions coming from the higher states and continuum are taken into account. These lead to the interval

$$11 \leq M^2 \leq 16 \text{ GeV}^2. \tag{15}$$

for both states. The pole dominance and OPE convergence are also considered in determination of the working region for the threshold parameter, which is obtained as

$$141 \leq s_0 \leq 145 \text{ GeV}^2 \tag{16}$$

for $J = \frac{3}{2}$ states with both parities and

$$142 \leq s_0 \leq 146 \text{ GeV}^2 \tag{17}$$

for $J = \frac{5}{2}$ states with negative and positive parities. Note that the above intervals for the continuum threshold are valid for both the b quark pole mass and running mass in the $\overline{\text{MS}}$ scheme. The calculation of the desired parameters of spin-5/2 states with the chosen interpolating current also requires determination of another auxiliary parameter, which is the mixing angle entering the interpolating current. We look for a working interval for this parameter such that our results depend on it relatively weakly. Our analyses show that the dependence of the results on $\cos\theta$ in the region $-0.5 \leq \cos\theta \leq 0.5$ for both the masses of the positive and negative parity pentaquarks with $J = \frac{5}{2}$ is weak (see Fig. 1). We use $\cos\theta$ to easily sweep the whole region by varying it in the interval $[-1, 1]$. It is worth noting that the pole quark mass together with the above intervals for the auxiliary parameters lead to maximally 78% and 79% pole contributions in spin-3/2 and spin-5/2 channels, respectively, which nicely satisfy the requirements of the QCD sum rules calculations.

As examples, the dependence of the masses and residues of the hidden bottom pentaquark states with spin-5/2 on M^2 at different fixed values of s_0 are shown in Figs. 2 and 3. From these figures it can be seen that the choices for the working intervals ensure the requirement of weak dependency of the results on these auxiliary parameters.

In this part, to see how the results depend on the b quark mass, as an example, we compare the mass of the pentaquark state with $J^P = \frac{3}{2}^+$ obtained via b quark pole mass (left panel) and b quark running mass in the $\overline{\text{MS}}$ scheme (right panel) as a function of s_0 at different fixed values of M^2 in Fig. 4. From this figure, it is obvious that

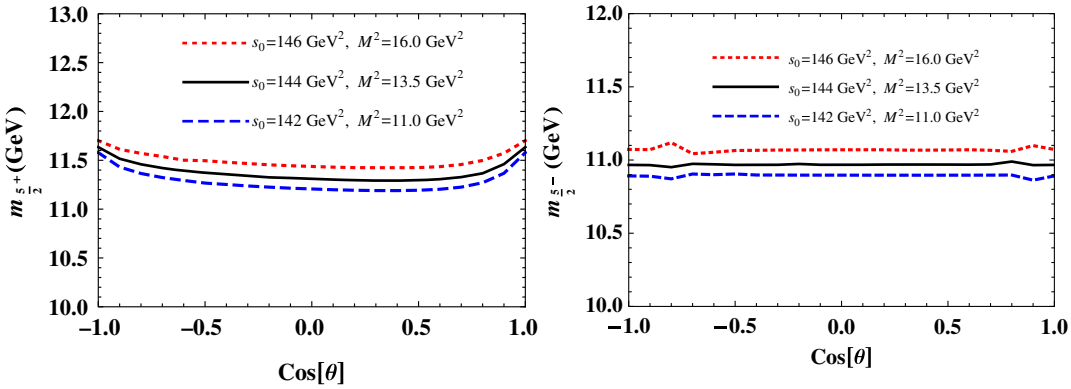

FIG. 1. (Left) Mass of the pentaquark with $J^P = \frac{5}{2}^+$ as a function of $\cos\theta$ at different fixed values of the continuum threshold and Borel parameter. (Right) Mass of the pentaquark with $J^P = \frac{5}{2}^-$ as a function of $\cos\theta$ at different fixed values of the continuum threshold and Borel parameter.

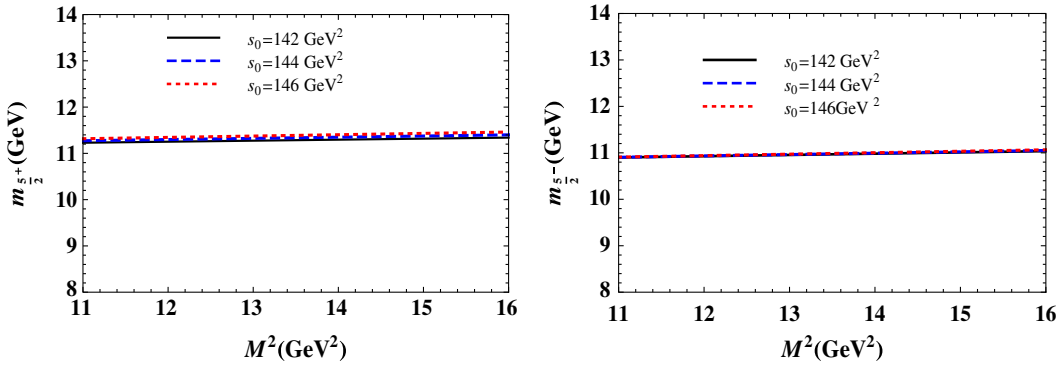

FIG. 2. (Left) Mass of the pentaquark with $J^P = \frac{5}{2}^+$ as a function of Borel parameter M^2 at different fixed values of the continuum threshold. (Right) Mass of the pentaquark with $J^P = \frac{5}{2}^-$ as a function of Borel parameter M^2 at different fixed values of the continuum threshold.

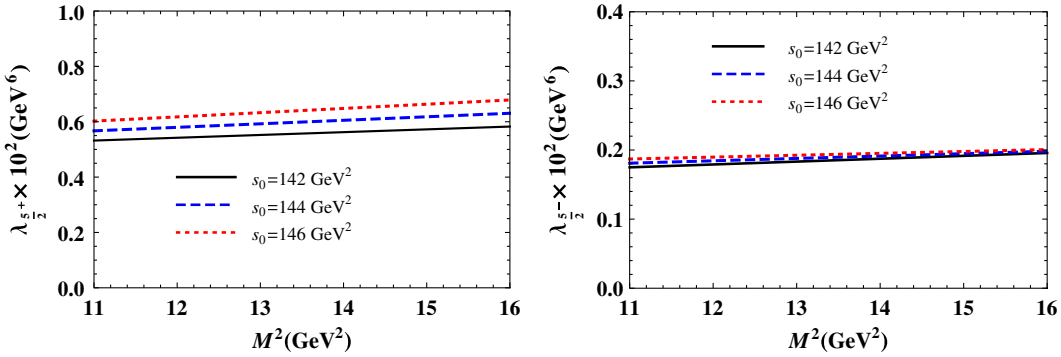

FIG. 3. (Left) Residue of the pentaquark with $J^P = \frac{5}{2}^+$ as a function of M^2 at different fixed values of the continuum threshold. (Right) Residue of the pentaquark with $J^P = \frac{5}{2}^-$ as a function of M^2 at different fixed values of the continuum threshold.

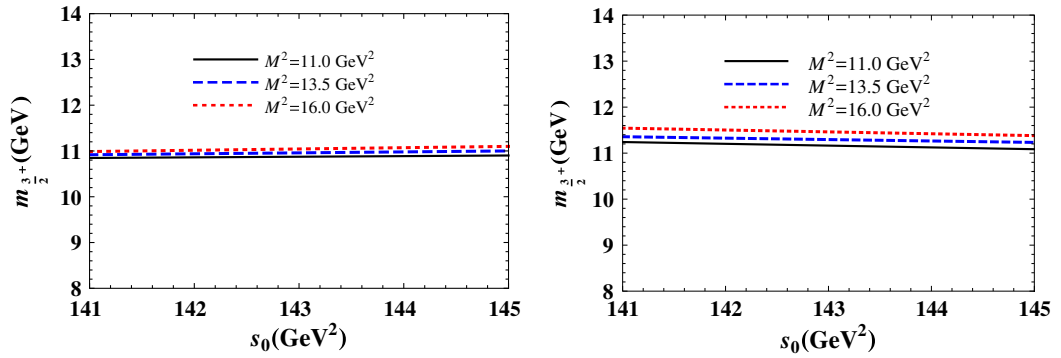

FIG. 4. (Left) Mass of the pentaquark with $J^P = \frac{3}{2}^+$ as a function of s_0 at different fixed values of M^2 using the b quark pole mass. (Right) Mass of the pentaquark with $J^P = \frac{3}{2}^+$ as a function of s_0 at different fixed values of M^2 using the b quark running mass.

the mass of this state changes with the amount of 3.2% on average when switching from the pole mass to the running mass. This amount becomes considerably larger in the case of residues. However, as is seen from this figure, the mass of this state is more stable with respect to the changes of the auxiliary parameters when the b quark pole mass is used compared to the case of b quark running mass. The masses of other states, and especially the residues of all particles under consideration, are also found to be more stable for the case of b quark pole mass.

Having established the intervals required for the auxiliary parameters M^2 and s_0, in the next step, these regions are applied to evaluate the masses m_{P_b} and residues λ_{P_b} of the states under consideration. In Table II, we provide the obtained results together with the corresponding errors that arise from the uncertainties inherited from the input parameters and the b

TABLE II. Results of QCD sum rules calculations for the mass and residue of the bottom pentaquark states.

J^P	m (GeV)	λ (GeV^6)
$\frac{3}{2}^+$	$10.93^{+0.82}_{-0.85}$	$(0.22^{+0.04}_{-0.04}) \times 10^{-2}$
$\frac{3}{2}^-$	$10.96^{+0.84}_{-0.88}$	$(0.36^{+0.05}_{-0.05}) \times 10^{-2}$
$\frac{5}{2}^+$	$11.94^{+0.84}_{-0.82}$	$(0.60^{+0.15}_{-0.16}) \times 10^{-2}$
$\frac{5}{2}^-$	$10.98^{+0.82}_{-0.82}$	$(0.19^{+0.04}_{-0.03}) \times 10^{-2}$

quark mass as well as those coming from fixing the working intervals of the auxiliary parameters. It is worth noting that, as is seen from Table II, there is a large mass splitting (∼960 MeV) between the central values of two opposite parities in the spin-$5/2$ channel compared to the ones of spin-$3/2$ states (∼30 MeV). This can be attributed to the different interpolating currents and internal structures used in these channels. For the spin-$3/2$ states we considered the molecular structure $\bar{B}^*\Sigma_b$, while for the spin-$5/2$ states we used the admixture of the $\bar{B}\Sigma_b^*$ and $\bar{B}^*\Lambda_b$ molecular structures with a mixing angle that we fixed later.

We would also like to compare our predictions with the existing results of other studies on $3/2^-$ and $5/2^+$ bottom pentaquarks states. In Ref. [33], the values for the masses are obtained as $m_{[\bar{B}^*\Sigma_b],3/2^-} = 11.55^{+0.23}_{-0.14}$ and $m_{[\bar{B}\Sigma_b^*\bar{B}^*\Lambda_b],5/2^+} = 11.66^{+0.28}_{-0.27}$ GeV. Though our predictions for the masses of these states are in agreement with the results of Ref. [33] considering the errors, the central value in our case is considerably lower (higher) for the $J^P = 3/2^-$ ($J^P = 5/2^+$) state compared to the predictions of Ref. [33]. Our results on the residues as well as the masses of the opposite-parity states can be checked via different theoretical approaches. The results of this work on the masses may shed light on future experimental searches, especially those at LHCb.

IV. SUMMARY AND OUTLOOK

In this work, the masses and residues of the hidden bottom pentaquarks with quantum numbers $J = 3/2$ and $J = 5/2$ and both the positive and negative parities have been computed using the QCD sum rule method. We adopted a molecular current of the $\bar{B}^*$ meson and Σ_b baryon to explore the states with $J = 3/2$, while a mixed molecular current of $\bar{B}$ meson and Σ_b^* baryon with $\bar{B}^*$ meson and Λ_b baryon were used to interpolate the states with $J = 5/2$ and both parities. After fixing the auxiliary parameters, namely, the continuum threshold and Borel parameter for both the spin-$3/2$ and spin-$5/2$ states, as well as the mixing parameter in the spin-$5/2$ channel, we found the numerical values of the masses and residues and compared the obtained results on the masses with the existing results of other theoretical studies. Although our predictions for the masses of the negative parity spin-$3/2$ and positive parity spin-$5/2$ states are nicely consistent with the results of Ref. [33] considering the uncertainties, the central value in our case is considerably low (high) for the $J^P = 3/2^-$ ($J^P = 5/2^+$) state compared to the predictions of Ref. [33]. Our results on the masses of the opposite-parity states as well as the residues can be verified via different theoretical studies. These results may shed light on the future experimental searches, especially those that are conducted at LHCb.

Our predictions for the masses of the considered states allow us to consider the decay modes like the S-wave $\Upsilon(1S)N$, $\Upsilon(2S)N$, $\Upsilon(1S)N(1440)$, $\Upsilon(1D)N$, and possibly $\bar{B}^*\Sigma_b$ decay channels for the spin-$3/2$ hidden bottom pentaquark states, as well as the S-wave $\Upsilon(1S)\Delta$, P-wave $\bar{B}^*\Lambda_b$, $\bar{B}^*\Sigma_b$, $\Upsilon(1S)N$, $\Upsilon(2S)N$, $\Upsilon(1s)N(1440)$, $\psi_{b1}(P)N$, $h_b(1P)N$, and D-wave $\Lambda_b B$ channels for the spin-$5/2$ decays. Investigation of these decay channels may provide valuable information for the experimental studies and help one to understand the structure of these particles, as well as their interaction mechanisms. We shall use our present results for the masses and residues of the pentaquarks in our future studies to analyze such strong decay channels.

ACKNOWLEDGMENTS

K. A. and Y. S. thank TÜBİTAK for partial support provided under the Grant No. 115F183. The work of H. S. was supported partly by BAP Grant No. 2017/018 of Kocaeli University. The authors would also like to thank S. S. Agaev for his useful discussions.

APPENDIX: SPECTRAL DENSITIES

As examples, in this Appendix, we present the perturbative and nonperturbative parts of the spectral densities corresponding to the structures $g_{\mu\nu}$ and $(g_{\mu\rho}g_{\nu\sigma} + g_{\mu\sigma}g_{\nu\rho})/2$ in terms of the integrals over the Feynman parameters x and y as follows:

$$\rho^{\mathrm{m,pert}}_{\frac{3}{2}}(s) = \frac{m_b}{5\times 2^{15}\pi^8}\int_0^1 dx \int_0^{1-x} dy \frac{(6sw - m_b^2 r)(sw - m_b^2 r)^4}{h^3 t^8}\Theta[L],$$

$$\rho^{m}_{\frac{3}{2},3}(s) = \frac{m_b^2}{2^9\pi^6}\langle\bar{d}d\rangle\int_0^1 dx \int_0^{1-x} dy \frac{(sw - m_b^2 t(x+y))^3}{h^2 t^5}\Theta[L],$$

$$\rho^{m}_{\frac{3}{2},4}(s)=\left\langle\frac{\alpha_s}{\pi}G^2\right\rangle\frac{1}{3^2\times2^{15}\pi^6}\int_0^1dx\int_0^{1-x}dy\frac{[sw-m_b^2t(x+y)]}{h^3t^7}\{12m_bswy^2(h^2sx^3+m_b^2t^2y)$$
$$-6m_by(m_b^2t(x+y)-sw)[2h^2sx^3y+m_b^2t^2y^2+hsx(34x^4+2y(y-1)^2(16y-9)$$
$$+x^3(105y-88)+x^2(72-209y+137y^2)+2x(50y^3-102y^2+61y-9))]$$
$$+m_b(sw-m_b^2t(x+y))^2[6h^2y^2+(68x^4+3y(y-1)^2(17y-12)$$
$$+x^3(197y-176)+8x^2(18-49y+31y^2)+3x(58y^3-123y^2+77y-12))]\}\Theta[L],$$

$$\rho^{m}_{\frac{3}{2},5}(s)=\frac{3m_b^2}{2^{10}\pi^6}m_0^2\langle\bar{d}d\rangle\int_0^1dx\int_0^{1-x}dy\frac{(sw-m_b^2t(x+y))^2}{ht^4}\Theta[L],$$

$$\rho^{m}_{\frac{3}{2},6}(s)=\frac{m_b}{3^3\times2^8\pi^6}(2g_s^2\langle\bar{u}u\rangle^2+g_s^2\langle\bar{d}d\rangle^2)\int_0^1dx\int_0^{1-x}dy\frac{x(m_b^2r-3sw)(m_b^2r-sw)}{t^5}\Theta[L]$$
$$+\frac{m_b}{2^4\pi^4}\langle\bar{u}u\rangle^2\int_0^1dx\int_0^{1-x}dy\frac{x(m_b^2r-3sw)(m_b^2r-sw)}{t^5}\Theta[L],$$

$$\rho^{\mathrm{m,pert}}_{\frac{5}{2}}(s)=\frac{m_b(5\cos^2\theta-4\cos\theta\sin\theta+12\sin^2\theta)}{2^{17}\times3\times5^2\pi^8}\int_0^1dx\int_0^{1-x}dy\frac{x(5x^2+x(y+5z)+5zy)}{h^3t^9}$$
$$\times(sw-m_b^2r)^4(m_b^2r-6sw)\Theta[L],$$

$$\rho^{m}_{\frac{5}{2},3}(s)=-\frac{m_b^2(\cos^2\theta(\langle\bar{d}d\rangle+4\langle\bar{u}u\rangle)+4\cos\theta\sin\theta(\langle\bar{d}d\rangle-2\langle\bar{u}u\rangle))}{2^{11}\times3^2\times\pi^6}\int_0^1dx\int_0^{1-x}dy\frac{(3x^2+x(y+3z)+3yz)}{h^2t^6}$$
$$\times(m_b^2r-sw)^3\Theta[L],$$

$$\rho^{m}_{\frac{5}{2},4}(s)=-\left\langle\frac{\alpha_s}{\pi}G^2\right\rangle\frac{m_b}{2^{17}\times3^3\times5\pi^6}\int_0^1dx\int_0^{1-x}dy\frac{x(m_b^2r-sw)}{h^3t^8}\{4\cos\theta\sin\theta(4s^2w^2(20x^6+100z^3y^3$$
$$+4x^5(31y+10z)+5xz^2y^2(56z+27y)+40x^3y(13-33y+20y^2)+x^4(20-504y+505y^2)+5x^2y$$
$$\times(219y-337y^2+154y^3-36))+m_b^4t^2(20x^8+10z^2y^5(22z+3y)+x^7(40z+314y)+x^6(20-1004y)$$
$$+1639y^2+2x^5y(475-2192y+1956y^2)+3xy^4(1095y-1232y^2+457y^3-320)+x^2y^3(6525y-8537y^2$$
$$+3572y^3-1560)+x^3y^2(-1120+6865y-11362y^2+5623y^3)+x^4y(-300+3865y-9221y^2+5779y^3))$$
$$-m_b^2sxy(100x^{10}+10z^4y^5(62z+9y)+10x^9(40y+93y)+xz^3y^4(2880-7505y+4733y^2)$$
$$+x^8(600-6220y+6633y^2)+x^2z^2y^3(23645y-4920-34196y^2+15489y^3)+x^7(11700y-400$$
$$-29884y^2+18857y^3)+x^3z^2y^2(-3680+29025y-56766y^2+31998y^3)+2x^6(50-5540y$$
$$+26777y^2-39055y^3+17777y^4)+2x^5y(2645-23834y+63097y^2-65643y^3+23735y^4)$$
$$+x^4y(-1020+21045y-98406y^2+183623y^3-151144y^4+45902y^5)))$$
$$+24\sin^2\theta(m_b^4t^2(20x^8+x^7(83z-17)-15z^2y^4(3y^2-2)+x^3y(120-750y+895y^2+256y^3-524y^4)$$
$$+x^6(170-398y+113y^2)-x^5(120-665y+623y^2+36y^3)+x^2y^2(180-630y+345y^2+541y^3-436y^4)$$
$$+x^4(30-470y+1080y^2-347y^3-332y^4)+xy^3(120-290y+20y^2+353y^3-203y^4))$$
$$+4s^2w^2(20x^6-30z^3y^2+4x^5(22z-3)+10xz^2y(6-11y+y^2)+x^4(170-318y+145y^2)$$
$$+5x^3(-24+86y-89y^2+27y^3)+10x^2(3-26y+50y^2-33y^3+6y^4))$$
$$-m_b^2sxy(100x^{10}+35x^9(19z-1)-15z^4y^4(8y+5y^2-10)+6x^8(325-690y+336y^2)$$
$$-2xz^3y^3(300-740y+300y^2+167y^3)+2x^7(-1400+5225y-5704y^2+1837y^3)$$
$$-x^3z^2y(5580y-11835y^2+6772y^3+319y^4-600)-x^2z^2y^2(4620y-6505y^2 2152y^3+642y^4$$
$$-900)+x^6(2200-13760y+26198y^2-19000y^3+4353y^4)+x^5(10005y-31216y^2+39533y^3-900$$
$$-20672y^4+3250y^5)+2x^4(75-1910y+10145y^2-20991y^3+19413y^4-7324y^5+592y^6)))$$

$$
\begin{aligned}
&+5\cos^2\theta(4s^2w^2(52x^6+4z^3y^2(5z-13)+4x^5(61z-1)+xz^2y(144-320y+107y^2)+x^4\\
&\times(412-864y+449y^2)-4x^3(72-284y+333y^2-121y^3)+x^2(72-660y+1419y^2-1129y^3+298y^4))\\
&+m_b^4t^2(52x^8+x^7(270z+22)-2z^2y^4(22y+29y^2)+x^6(412-1156y+599y^2-36)\\
&+2x^5(893y-1186y^2+348y^3-144)+x^2y^2(432-1824y+2133y^2-409y^3-332y^4)\\
&+x^3y(288-2024y+3521y^2-1658y^3-133y^4)-3xy^3(296y-235y^2-36y^3+71y^4-96)\\
&+x^4(72-1188y+3365y^2-2677y^3+359y^4))-m_b^2sxy(260x^{10}+2x^9(-880+931y)\\
&-2z^4y^4(206y+19y^2-180)+5x^8(960-2236y+1233y^2)+xz^3y^3(4128y-2941y^2-1440\\
&+145y^3)+x^7(27420y-33356y^2+12589y^3-6800)+x^2z^2y^2(2160-12072y+20341y^2-12004y^3\\
&+1557y^4)+x^3z^2y(1440-14128y+34209y^2-27606y^3+5634y^4)+2x^6(2650-17620y\\
&+36793y^2-30611y^3+8779y^4)+2x^5(12535y-42226y^2+60059y^3-37935y^4+8647y^5-1080)\\
&+x^4(360-9372y+52905y^2-120438y^3+129907y^4-65384y^5+12022y^6))))\}\Theta[L],
\end{aligned}
$$

$$
\rho^m_{\frac{5}{2},5}(s)=\frac{(\cos\theta-2\sin\theta)m_b^2m_0^2(6\sin\theta\langle\bar{d}d\rangle+\cos\theta(\langle\bar{d}d\rangle+4\langle\bar{u}u\rangle))}{2^{13}\pi^6}\int_0^1dx\int_0^{1-x}dy\frac{(sw-m_b^2t(x+y))^2}{ht^5}
$$

$$
\times(2x^2+x(3z+1)+2yz)\Theta[L],
$$

$$
\begin{aligned}
\rho^m_{\frac{5}{2},6}(s)=&\int_0^1dx\int_0^{1-x}dy\Big\{(2g_s^2\langle\bar{u}u\rangle^2+g_s^2\langle\bar{d}d\rangle^2)\frac{m_b(5\cos^2\theta-4\cos\theta\sin\theta+12\sin^2\theta)}{2^{11}\times3^4\pi^6}(m_b^2t(x+y)-3sw)\\
&\times(m_b^2t(x+y)-shxy)(2xyz+x^2(2x+3y-2))-\frac{m_b(\cos\theta-2\sin\theta)}{3\times2^8\pi^4t^5}[\langle\bar{u}u\rangle^2(\cos\theta+6\sin\theta)+4\langle\bar{u}u\rangle\langle\bar{d}d\rangle\cos\theta]\\
&\times(m_b^2tx(x+y)-3swx)(m_b^2t(x+y)-sw)\Big\}\Theta[L],
\end{aligned}
\tag{A1}
$$

where $\Theta[L]$ is the usual unit-step function and we have used the shorthand notations

$$
\begin{aligned}
&z=y-1,\qquad h=x+y-1,\qquad t=x^2+(x+y)(y-1),\qquad r=x^3+x^2(2y-1)+y(y-1)(2x+y),\\
&w=hxy,\qquad L=\frac{z}{t^2}[sw-m_b^2(x+y)t].
\end{aligned}
\tag{A2}
$$

[1] R. Aaij *et al.* (LHCb Collaboration), Phys. Rev. Lett. **115**, 072001 (2015).
[2] K. Azizi, Y. Sarac, and H. Sundu, Phys. Rev. D **95**, 094016 (2017).
[3] R. L. Jaffe, Phys. Rev. D **15**, 267 (1977).
[4] C. Gignoux, B. Silvestre-Brac, and J. M. Richard, Phys. Lett. B **193**, 323 (1987).
[5] H. Hogaasen and P. Sorba, Nucl. Phys. **B145**, 119 (1978).
[6] D. Strottman, Phys. Rev. D **20**, 748 (1979).
[7] H. J. Lipkin, Phys. Lett. B **195**, 484 (1987).
[8] S. Fleck, C. Gignoux, J. M. Richard, and B. Silvestre-Brac, Phys. Lett. B **220**, 616 (1989).
[9] Y. S. Oh, B. Y. Park, and D. P. Min, Phys. Lett. B **331**, 362 (1994).
[10] C. K. Chow, Phys. Rev. D **51**, 6327 (1995).
[11] M. Shmatikov, Nucl. Phys. **A612**, 449 (1997).
[12] M. Genovese, J. M. Richard, F. Stancu, and S. Pepin, Phys. Lett. B **425**, 171 (1998).
[13] H. J. Lipkin, Nucl. Phys. **A625**, 207 (1997).
[14] D. B. Lichtenberg, J. Phys. G **24**, 2065 (1998).
[15] H. C. Kim, M. V. Polyakov, and M. Praszaowicz, Phys. Rev. D **96**, 014009 (2017).
[16] R. Aaij *et al.* (LHCb Collaboration), Phys. Rev. Lett. **118**, 182001 (2017).
[17] J. He, Phys. Rev. D **95**, 074031 (2017).
[18] G. J. Wang, R. Chen, L. Ma, X. Liu, and S. L. Zhu, Phys. Rev. D **94**, 094018 (2016).
[19] R. Zhu and C. F. Qiao, Phys. Lett. B **756**, 259 (2016).
[20] R. F. Lebed, Phys. Lett. B **749**, 454 (2015).
[21] V. V. Anisovich, M. A. Matveev, J. Nyiri, A. V. Sarantsev, and A. N. Semenova, arXiv:1507.07652.
[22] L. Maiani, A. D. Polosa, and V. Riquer, Phys. Lett. B **749**, 289 (2015).

[23] R. Ghosh, A. Bhattacharya, and B. Chakrabarti, arXiv:1508.00356.
[24] Z. G. Wang and T. Huang, Eur. Phys. J. C **76**, 43 (2016).
[25] Z. G. Wang, Eur. Phys. J. C **76**, 70 (2016).
[26] Z. G. Wang, Nucl. Phys. **B913**, 163 (2016).
[27] L. Roca, J. Nieves, and E. Oset, Phys. Rev. D **92**, 094003 (2015).
[28] R. Chen, X. Liu, X. Q. Li, and S. L. Zhu, Phys. Rev. Lett. **115**, 132002 (2015).
[29] H. Huang, C. Deng, J. Ping, and F. Wang, Eur. Phys. J. C **76**, 624 (2016).
[30] U. G. Meißner and J. A. Oller, Phys. Lett. B **751**, 59 (2015).
[31] C. W. Xiao and U.-G. Meißner, Phys. Rev. D **92**, 114002 (2015).
[32] J. He, Phys. Lett. B **753**, 547 (2016).
[33] H. X. Chen, W. Chen, X. Liu, T. G. Steele, and S. L. Zhu, Phys. Rev. Lett. **115**, 172001 (2015).
[34] R. Chen, X. Liu, and S. L. Zhu, Nucl. Phys. **A954**, 406 (2016).
[35] Y. Yamaguchi and E. Santopinto, Phys. Rev. D **96**, 014018 (2017).
[36] J. He, Phys. Rev. D **95**, 074004 (2017).
[37] N. N. Scoccola, D. O. Riska, and M. Rho, Phys. Rev. D **92**, 051501 (2015).
[38] H. X. Chen, W. Chen, X. Liu, and S. L. Zhu, Phys. Rep. **639**, 1 (2016).
[39] Y. Shimizu, D. Suenaga, and M. Harada, Phys. Rev. D **93**, 114003 (2016).
[40] Y. Liu and I. Zahed, arXiv:1704.03412.
[41] T. Sakai and S. Sugimoto, Prog. Theor. Phys. **113**, 843 (2005).
[42] J.-J. Wu, R. Molina, E. Oset, and B. S. Zou, Phys. Rev. Lett. **105**, 232001 (2010).
[43] J.-J. Wu, L. Zhao, and B. S. Zou, Phys. Lett. B **709**, 70 (2012).
[44] F. K. Guo, U. G. Meisner, W. Wang, and Z. Yang, Phys. Rev. D **92**, 071502 (2015).
[45] X. H. Liu, Q. Wang, and Q. Zhao, Phys. Lett. B **757**, 231 (2016).
[46] F. K. Guo, U. G. Meisner, J. Nieves, and Z. Yang, Eur. Phys. J. A **52**, 318 (2016).
[47] M. Bayar, F. Aceti, F. K. Guo, and E. Oset, Phys. Rev. D **94**, 074039 (2016).
[48] M. A. Shifman, A. I. Vainshtein, and V. I. Zakharov, Nucl. Phys. **B147**, 385 (1979).
[49] M. A. Shifman, A. I. Vainshtein, and V. I. Zakharov, Nucl. Phys. **B147**, 448 (1979).